JETIR.ORG ISSN: 2349-5162 | ESTD Year : 2014 | Monthly Issue
JOURNAL OF EMERGING TECHNOLOGIES AND INNOVATIVE RESEARCH (JETIR)
An International Scholarly Open Access, Peer-reviewed, Refereed Journal

Effect of Ni^{2+} ions on the structural, morphological and optical properties of microwave-assisted synthesis of ZnO nanoparticles

P. Prabukanthan, K. Mageswari

Materials Chemistry Lab, Department of Chemistry, Muthurangam Government Arts College, Vellore 632002, India.

Abstract: Zn1-xNixO nanoparticles with Ni^{2+} ions concentration x = 1 to 5 mole % were synthesised by microwave-assisted technique. The structural, morphological and optical properties were analyzed as a function of the Ni^{2+} ion concentration. The XRD illustrate the increases in crystallinity of ZnO nanoparticles with increases of Ni^{2+} ions concentration and doped systems at various Ni^{2+} ions mole fractions x confirmed the exclusive formation of the host ZnSe with the hexagonal wurtzite structure. The SEM results show that nanorods having nanoscale diameter and length were successfully synthesized by microwave-assisted technique. The UV–visible spectroscopy verified that the band gap of ZnO was reduced due to incorporation of Ni into ZnO. Photoluminescence (PL) spectra of 1 to 5 mole % Ni^{2+} ion doped ZnO nanoparticles show two distinct ZnO and Ni^{2+} related emissions, both of which are excited via the ZnO host lattice. PL spectra confirmed a huge enhanced deep-level emission which attributes to the increase in defects concentration due to Ni^{2+} ions doping.

I. INTRODUCTION

Due to increasing environment pollution, the quest for low cost and highly visible light active photocatalyst for efficient environmental remediation has emerged as an important area of research. Therefore, semiconductor based nanostructured materials have attained a lot of attention as a potential photocatalyst [1-2]. To arrest ecological deterioration, semiconducting photocatalysis was applied to deal with a variety of environmental problems such as purification of polluted water and air. Among different semiconductor materials, metal oxide such as TiO_2, ZnO, WO_3, Cu_2O and ZrO_2 have been intensively investigated as photocatalysts due to their high photocatalytic activity, non-toxicity, good stability and low cost [3-4]. Especially, ZnO is a suitable alternative photocatalyst to TiO_2 because of its distinct advantages including the direct band gap, ease of crystallization, and higher exciton binding energy and electron mobility [5]. However, the photocatalytic efficiency remains very low because of the fast recombination rate of the photogenerated electron-hole pairs in ZnO [6].

In this context, conventional nanostructured based photocatalyst including ZnO with wide band (Eg = 3.37 eV at 300 K) is still considered as the most exceptional photocatalyst option due to its outstanding optical properties, environmental sustainability and low cost [7–10]. However, the photocatalytic performance of ZnO is low due to low visible light absorption and high recombination rate of electron hole pairs which is the main obstacle for its utilization at commercial level [8]. To tackle these problems different methods could be applied such as doping with metals, non-metals, co-doping, and making composites/hybrids [11].

Herein, we prepared Zn1-xNixO nanoparticles with Ni^{2+} ions concentration x = 1 to 5 mole % by simple, scalable, and environmental friendly microwave-assisted technique. The structure, morphologies with composition and luminescence properties of Zn1-xNixO nanoparticles were by X-ray diffraction (XRD), scanning electron microscopy with EDAX and photoluminescence intensively investigated and reported.

2. EXPERIMENTAL SECTION

Zinc nitrate, nickel nitrate and NaOH, material were sourced from Sigma-Aldrich. All these chemicals and reagents were utilized as received.

2.1 Synthesis of Zn1-xNixO nanoparticles

Zn1-xNixO nanoparticles with Ni^{2+} ions concentration x = 1 to 5 mole % were synthesized by using microwave irradiation method. The synthesis solution was prepared by mixing of 100 ml of 0.5 moldm-3 zinc nitrate 10 ml of (1 to 5 mole %) nickel nitrate taken in a beaker containing 250 ml of deionized water, to this mixture 0.1 N NaOH was added with constant stirring at room temperature and the mixture was subjected to microwave irradiation at 400 w for 30 min [12]. Finally, the obtained white precipitate (ZnO) and light green precipitate (Zn1-xNixO) was washed with water and ethanol several times followed by during about 200 °C for 10-15 min.

2.2 Characterization

X-ray diffraction (XRD) patterns obtained from Plus/D8 model X-ray diffract-meter under Cu Kα radiation at scan rate of 10° per min. The surface morphology with chemical composition of samples was tested through scanning electron microscope (SEM) with energy dispersive X-ray analysis (EDAX) using Hitachi-S-4300SE with equipped voltage of 10 kV. The optical absorbance spectra of Zn1-xNixO nanoparticles were recorded using Shimadzu UV–visible spectrometer in the range 200–2000 nm. The luminescence properties were investigated using a PL Mechelle 900 spectrograph in the range 300–1100 nm, using a 325 nm He–Cd laser as an excitation source at room temperature.

3.RESULTS AND DISCUSSION

3.1 XRD analysis

Fig. 1 shows the powder X-ray diffraction (XRD) patterns of Zn1-xNixO nanoparticles with Ni2+ ions concentration x = 1 to 5 mole %. All peak positions of the nanoparticles correspond to the standard diffraction pattern of hexagonal wurtzite structure ZnO. Fig. 1 the XRD pattern of ZnO shows the diffraction peaks at 2θ = 31.9°, 34.7°, 36.5°, 47.7°, 56.8°, 63.0°, 66.3°, 67.9°, 69.1°, 73.1 and 77.0° and corresponds to (100), (002), (101), (102), (110), (103), (200), (112), (201), (004) and (202) diffraction planes. The absence of extra peaks in these XRD patterns suggests that the Zn1-xNixO nanoparticles are the actual substitution of dopant into the host wurtzite structure, absence of impurities and also no precipitates or large-sized clusters are present in these nanoparticles [13].

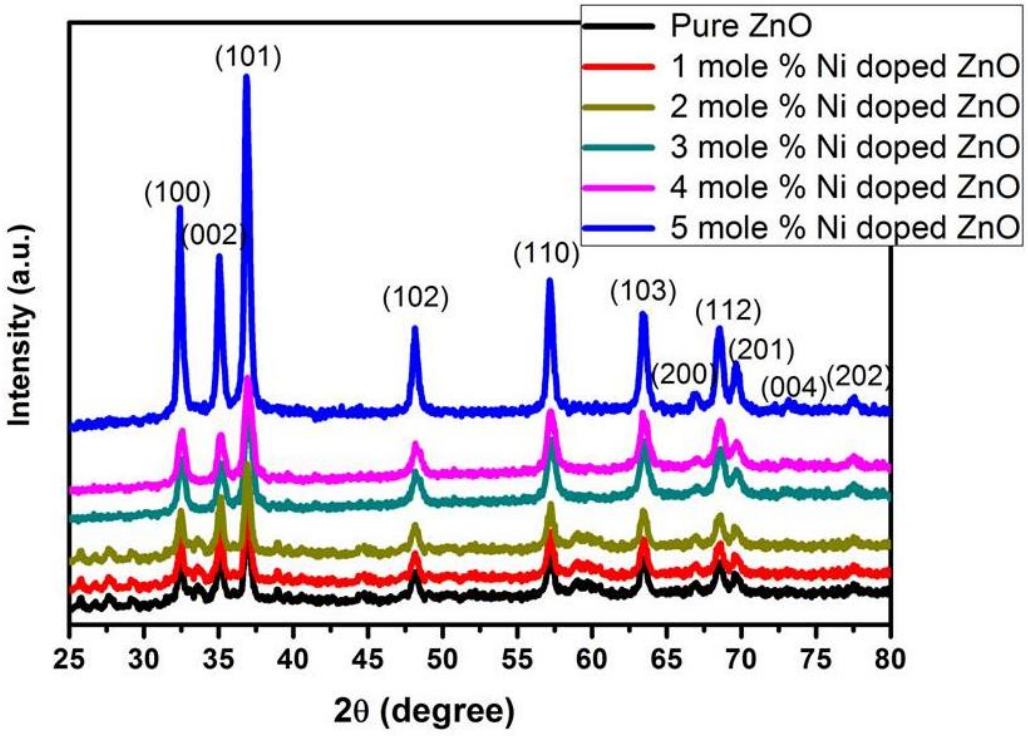

Fig. 1. XRD spectra of $Zn_{1-x}Ni_xO$ nanoparticles

The XRD peak intensity increased with increase in the concentrations of Ni2+ ions due to elevation of crystallinity. From the high intensity (101) plane, the lattice constants a and c were evaluated using the relation,

$$\frac{1}{d_{hkl}^2} = \frac{4}{3}\left[\frac{h^2 + hk + l^2}{a^2}\right] + \frac{l^2}{c^2} \quad (1)$$

where, h,k,l are miller indices and dhkl is distance between the crystallographic planes and these values are presented in Table 1. As the effective ionic radius of Ni2+ (0.68 Å) is smaller than that of Zn2+ (0.72 Å) the lattice constant would increase with increased Ni2+ substitution. However, Ni2+ doped ZnO nanoparticles retain the wurtzite crystal structure of ZnO suggesting that nickel substitution at such low concentrations does not alter the crystal structure.

The Debey Scherrer formula given by the following relation was used to calculate the crystallite size of the Zn1-xNixO nanoparticles.

$$D = K\,\lambda/(\beta\cos\theta) \quad (2)$$

where; D is the average crystallite size of Zn1-xNixO nanoparticles, K is Scherrer constant it is the shape factor (dimensionless shape factor has a typical value about 0.9), β is the full width half maximum of the diffraction peak in radians or integral breadth, θ representing diffraction Bragg angle (in degree) and λ representing the wavelength of X-ray beam (1.5406 A°). The calculated average crystallite sizes were found to be in the range of 200-400 nm and are listed in Table 1. The crystalline sizes reveal that there is increase in the crystalline size while increasing Ni2+ ions concentrations. SEM analysis showed that there was a strong line between these results is shown in Fig. 2.

Table 1 FWHM, lattice parameters, crystallite size, composition of $Zn_{1-x}Ni_xO$ nanoparticles by XRD and EDAX.

Samples	FWHM of XRD peak (101) (deg.)	Lattice parameters (Å)		Crystalline size (nm)	Composition (atomic %)		
		a	c		Zn	O	Ni
Pure ZnO	0.4251	3.29	5.18	198	49.59	50.41	0
1 mole % Ni^{2+} doped ZnO	0.4397	3.31	5.19	232	48.74	50.27	0.98
2 mole % Ni^{2+} doped ZnO	0.4512	3.35	5.19	244	46.83	50.18	2.99
3 mole % Ni^{2+} doped ZnO	0.4615	3.36	5.21	289	46.77	50.22	3.01
4 mole % Ni^{2+} doped ZnO	0.4719	3.39	5.22	321	45.61	50.41	3.98
5 mole % Ni^{2+} doped ZnO	0.4899	3.41	5.29	402	45.1	50.12	4.78

3.2 Morphological analysis

Surface morphology of the pristine and irradiated films was studied by SEM. The SEM images of the Zn1-xNixO nanoparticles are shown in Fig. 2 (a)–(f). The Zn1-xNixO nanoparticles SEM images are not uniform with a wide range of grain sizes but hexagonal shape was appeared also nickel concentration was increases the size of hexagonal shape also increased.

The composition analysis of the Zn1-xNixO nanoparticles was carried using energy dispersive X-ray analysis (EDAX) spectral data of different regions of the nanoparticles recorded with an incident electron beam of 20 keV. Fig. 3 (a-c) shows the EDAX results of pure, 3 and 5 mole % Ni^{2+} doped ZnO nanoparticles. The results of the corresponding elements in atomic percentage are given in Table 1. Pure ZnO in the Fig. 3a shows that the relative proportions expressed in the atomic elementals ratio for O:Zn were, 1.00:1.00, which is consistent with the theoretical stoichiometry of ZnO. The stoichiometric oxygen content suggests absence of oxygen vacancies, which may noticeably alter the aggregate optical and electronic properties of the nanoparticles. The EDAX spectra of 3 and 5 mole % of Ni^{2+} doped ZnO nanoparticles shown in Fig. 3 (b-c) indicated that it contained Ni, Zn and O elements. From Table 1, there is a deviation in the compositions of Zn is observed, when the concentration of nickel increases in ZnO nanoparticles. These results indicate that Ni might act as a substitute at a Zn site in the ZnO system, suggesting that there could be the formation of Zn1-xNixO compounds [14-15].

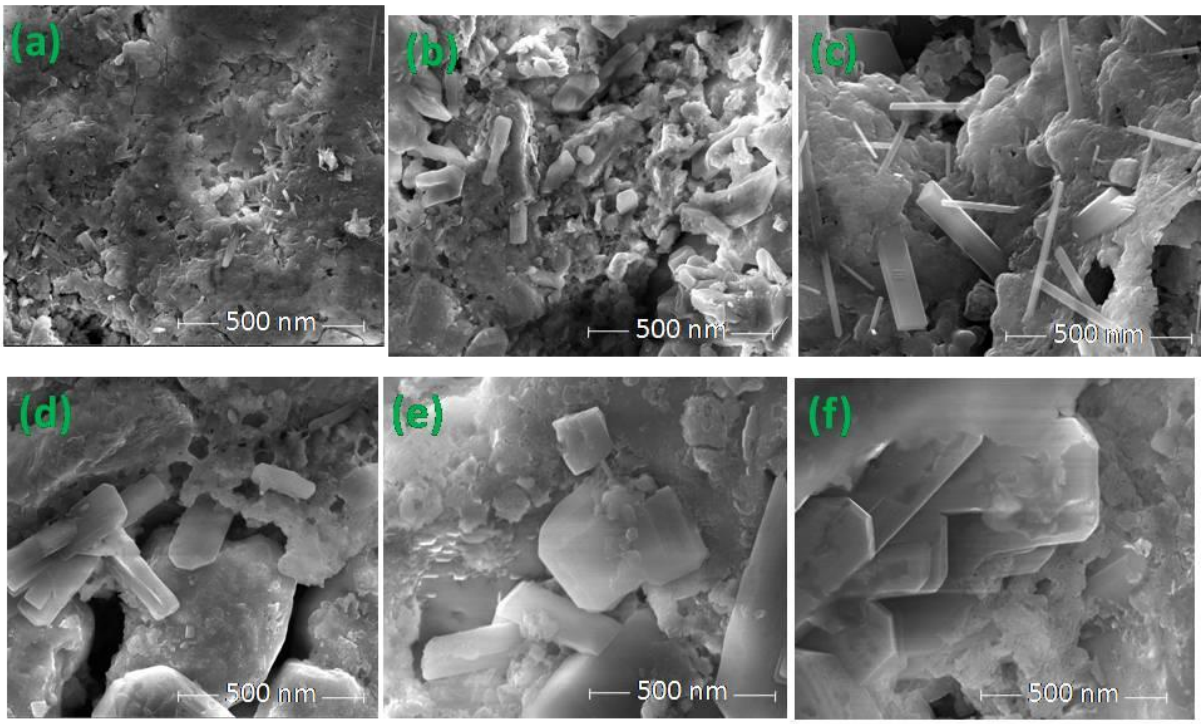

Fig. 2 SEM images of Ni^{2+}doped ZnO nanoparticles with unposed (a), 1 (b), 2 (c), 3 (d), 4 (e) and 5 (f) mole % Ni^{2+} ions.

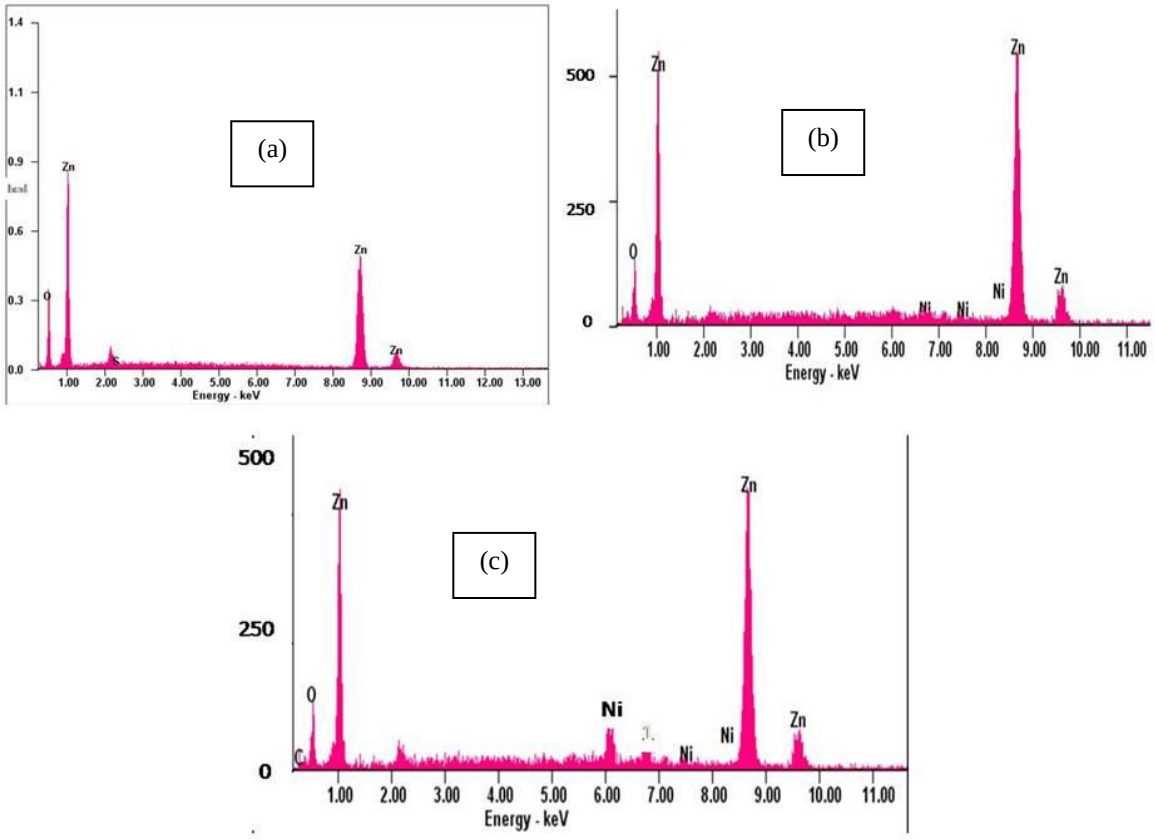

Fig. 3 EDAX spectra of Ni^{2+}doped ZnO nanoparticles with unposed (a), 3 (b), and 5 (c) mole % Ni2+ ions.

3.3 UV-Vis DRS analysis

Fig. 4 shows the UV-vis DRS spectra of Zn1-xNixO nanoparticles optical absorption spectra is considered a versatile tool to reveal electronic transition, when Ni^{2+} ions are incorporated into ZnO lattice and substituting for Zn^{2+} at tetrahedral sites of the ZnO wurtzite structure. In the spectra of Ni^{2+} doped films absorption edge is slightly red shifted compared to pure ZnO compound and this in the absorption edge towards lower energy indicates that incorporation of Ni^{2+} ions in ZnO lattice reduces the band gap [15]. Absorption spectra of pure ZnO shows only a sharp absorption edge, but the doping of Ni^{2+} ions in the concentration of 1,2 3, 4 and 5 mole % into ZnO lattice leads clearly to the appearance of one well defined additional absorption peak at 273 nm, 295nm, 272 nm, 302 nm, and 296 nm, respectively. This additional peak may be related to the d-d transitions of Ni^{2+} ions involving crystal filed levels in tetrahedral crystal symmetry. But the relative intensity of this additional peak does change with 3 mole % nickel concentration [16].

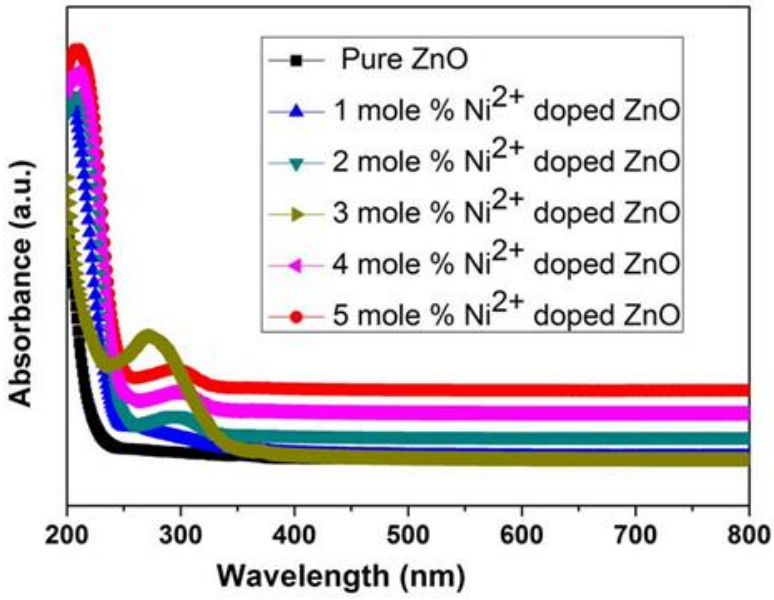

Fig. 4 Optical absorbance spectra of Zn1-xNixO nanoparticles

3.4Photoluminescence analysis

Photoluminescence (PL) measurements of Zn1-xNixO nanoparticles were carried out to investigate the luminescent characteristics in the visible region at room temperature as shown in Fig. 5. The measurement conditions were identical in all cases and therefore relative intensities can be compared. The PL spectra for the pure ZnO nanoparticles showed that the strong broad emission band at 478 nm is attributed to the band-band gap luminescence. Two PL emission lines are observed for 1 to 3 mole %

Ni^{2+} ions doped ZnO nanoparticles. The high intensity and strong PL emission lines are at the different position for the 1 to 5 mole % Ni^{2+} ions doped ZnO nanoparticles. Although the radii of Ni^{2+} ions (0.68 Å) seem to be too smaller to allow them to replace Zn^{2+} ions (0.72 Å) in cubic crystal lattice. With the increase of Ni^{2+} ions doping concentration, the emission intensity showed decreases 4 to 5 mole % Ni^{2+} ions concentration, but shape and position of this peak did obviously change during this process [17]. We suppose that the lattice vibrations induced by Ni^{2+} ions in single tracks help to the reorientation of these areas and minimization of inter-facial energy between ZnO grains. For the 4 to 5 mole % Ni^{2+} ions concentration ZnO samples, the intensity of the luminescence peak is lower compared to the pure ZnO indicating loss of luminescent property of the ZnO compound after Ni^{2+} ions concentration. This further confirms the increased crystal lattice size on the interfacial surface of the sample due to Ni^{2+} ions concentration [18].

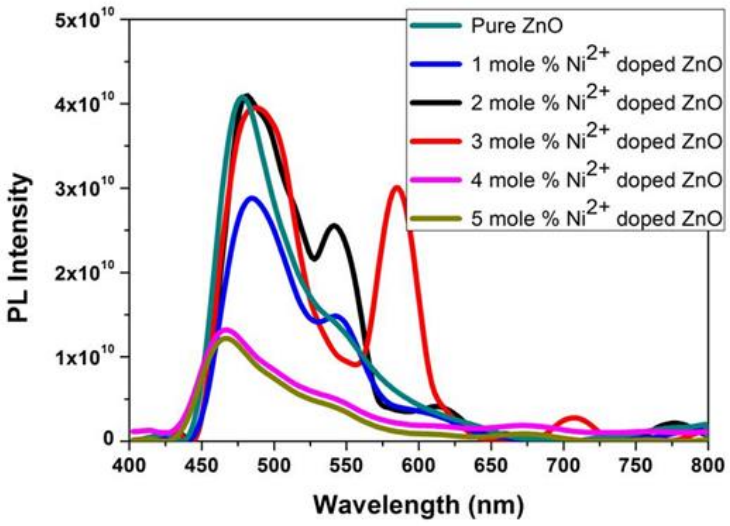

Fig. 5 Photoluminescence spectra of Zn1-xNixO nanoparticles

4.Conclusions

A good quality single crystalline nanoparticle of ZnO doped with Ni^{2+} in various concentrations has been successfully synthesized from microwave irradiation technique.

The XRD patterns confirm that pure and Ni^{2+} doped ZnO crystallizes in the hexagonal wurtzite structure phase without any precipitated (secondary phase) dopant related phase. Lattice parameters 'a' and 'c' show variation (increasing) by increasing the substitution level of Ni^{2+} ions in ZnO, indicating the substitution of dopant Ni^{2+} into Zn^{2+} positions in the ZnO lattice. The fundamental absorption edge of the Ni^{2+} into ZnO nanoparticles show a large change due to Ni^{2+} incorporated into the ZnO lattice. The crystallinity and surface structure of the nanoparticles strongly influence the optical properties. Thus the stronger PL intensity Zn1-xNixO nanoparticles could be attributed to the increases grain size.

REFERENCES

[1] Shoaib A. Fahad S.A.K. Nabisab M.M. Mohammad K. Yie H.T. Shaukat A.M. Rama R.Kand Ezzat C.A. 2021. Emerging pollutants and their removal using visible-light responsive photocatalysis – A comprehensive review. Journal of Environmental Chemical Engineering, 9(6): 106643.

[2] Muhammad S. Usama A. TahaT.A. Qazi H.I.A. Abdullah G. Al S. Sami U. Hamed A. AhmedI.M. Mohammed A. Amin A. P. Waseem I. Sarah A. NawawiW.I. Zeeshan A. Hamid A. Asif H. 2022. Nanostructured materials based on g-C3N4 for enhanced photocatalytic activity and potentials application: A review. Arabian Journal of Chemistry, 15(9): 104070.

[3]Shraddha S. Himanshu P. Prashansha S. Anish K.T. Vikas B. and Avinash C.P. 2021, Synergistic impact of photocatalyst and dopants on pharmaceutical-polluted waste water treatment: a review. Environmental Pollutants and Bioavailability 33(1): 347-364.

[4]Nunes D. Pimentel A. Branquinho R. Fortunato E. and Martins R. 2021. Metal Oxide-Based Photocatalytic Paper: A Green Alternative for Environmental Remediation. Catalysts, 11: 504.

[5]Mujeeb K. Mohamed E. Assal M.N.T. Majad K. Muhammad A. Mohammad R.H. Merajuddin K. Ravi V. Nujud M.B. and Syed F.A. 2022. Graphene/inorganic nanocomposites: Evolving photocatalysts for solar energy conversion for environmental remediation. Journal of Saudi Chemical Society, 26(6): 101544.

[6]Chin B.O. Law Y.N. and Abdul W.M. 2018. A review of ZnO nanoparticles as solar photocatalysts: Synthesis, mechanisms and applications, Renewable and Sustainable Energy Reviews, 81 (1): 536-551.

[7]Tahir M.B. Nabi G. Khalid N.R. and Khan W.S.,2018. Synthesis of Nanostructured Based WO_3 Materials for Photocatalytic Applications. J. Inorg. Organomet. Polym. Mater 28 (3): 777–782.

[8]Ibrahim K. Khalid S. and Idrees K. 2019. Nanoparticles: Properties, applications and toxicities. Arabian Journal of Chemistry, 12 (7): 908-931.

[9]Shunyu Y. Xu Z. Fengyu Q. Ahmad U. and Xiang W. 2016. Hierarchical WO_3 nanostructures assembled by nanosheets and their applications in wastewaterpurification. J. Alloys Compd. 1–21.

[10]Mao T. Liu M. Lin L. Cheng Y. and Fang, C. 2022. A Study on Doping and Compound of Zinc Oxide Photocatalysts. Polymers 14: 4484.

[11]Alhebshi A. Sharaf A.E. Mim R.S. Tahir B. and Tahir M. 2022. Recent advances in constructing heterojunctions of binary semiconductor photocatalysts for visible light responsive CO_2 reduction to energy efficient fuels: A review. Int J Energy Res. 46(5): 5523- 5584.

[12]Mageswari K. Prabukanthan P. and Madhavan J. 2023. Microwave-assisted synthesis of ZnO nanoparticles using different capping agents and their photocatalytic application. Environ Sci Pollut Res https://doi.org/10.1007/s11356-022-25097-9.

[13] Prabukanthan P. and Harichandran G.2013. Effect of 100 MeV O^{7+} ion beam irradiation on radio frequency reactive magnetron sputtered ZnO thin films. Materials Science in Semiconductor Processing, 16: 193-199.

[14]Mihalache V. Negrila C. Bercu V. Secu M. Vasile E. and Stan G.E. 2019. Effect of dilute doping and non-equilibrium synthesis on the structural, luminescent and magnetic properties of nanocrystalline Zn1-xNixO (x = 0.0025 – 0.03). Materials Research Bulletin, 115: 37-48.

[15] Prabukanthan P. Sreedhar M. Thamaraiselvi S. Harichandran G. Seenuvasakumaran P. Marlia M. Hanafiah and Carlos F. 2021. Photoelectrochemical applications of electrochemical deposition of Ni^{2+}-doped FeS_2 thin films. J Mater Sci: Mater Electron 32: 6331-6343.

[16] Ali H. Alsmadi A.M. Salameh B. Mathai M. Shatnawi M.Hadia N.M.A.and IbrahimE.M.M. 2020. Influence of nickel doping on the energy band gap, luminescence, and magnetic order of spray deposited nanostructured ZnO thin films. Journal of Alloys and Compounds 816: 152538.

[17]Prabukanthan P.and Dhanasekaran R. 2008, Influence of Mn doping on $CuGaS_2$ single crystals grown by CVT method and their characterization. Journal Physics D: Applied Physics 41:115102.

[18] Rajesh Kumar T. Prabukanthan P. Harichandran G. Senthil R.A. Arunkumar T. and Theerthagiri J. 2019. A simple, economical, and quick electrochemical deposition of rare-earth metal ion–doped ZnSe/FeS_2 double-layer thin films with enhanced photoelectrochemical performance. Ionics 25: 6115–6122.